

# Reservoir modelling of heterolithic tidal deposits: sensitivity analysis of an object-based stochastic model

C.R. Geel\* & M.E. Donselaar

Department of Geotechnology, Delft University of Technology, P.O. Box 5048, 2600 GA Delft, the Netherlands.

\* Corresponding author. Present address: TNO Built Environment and Geosciences, *Geological Survey of the Netherlands*, P.O. Box 80015, 3508 TA Utrecht, the Netherlands. Email: kees.geel@tno.nl

Manuscript received: October 2007; accepted: December 2007

## Abstract

Object-based stochastic modelling techniques are routinely employed to generate multiple realisations of the spatial distribution of sediment properties in settings where data density is insufficient to construct a unique deterministic facies architecture model. Challenge is to limit the wide range of possible outcomes of the stochastic model. Ideally, this is done by direct validation with the 'real-world' sediment distribution. In a reservoir setting this is impossible because of the limited data density in the wide-spaced wells. In this paper this uncertainty is overcome by using size, shape and facies distributions of tidal channel and tidal flat sand bodies in a highly data-constrained lithofacies architecture model as input for the object-based stochastic model. The lithofacies architecture model was constructed from a densely perforated (Cone Penetration Tests and cored boreholes) tidal estuarine succession of the Holocene Holland Tidal Basin in the Netherlands. The sensitivity of the stochastic model to the input parameters was analysed with the use of varying tidal channel width and thickness values and calculating the connected sand volume per well for the different scenarios. The results indicated that for a small well drainage radius the difference in drainable volumes between the narrowest and the widest channel scenarios is large, and that for a large well drainage radius the tidal channel width hardly influenced the drainable volume. The sensitivity analysis highlighted the importance of sand-dominated tidal flats in improving lateral connectivity.

**Keywords:** Object-based stochastic modelling, sensitivity analysis, heterolithic tidal deposits

## Introduction

Tidal estuarine basins show a highly heterogeneous distribution of sand and mud sediment. Sand is concentrated by high-energy currents in tidal channels and creeks. Dissipation of tidal energy along the branching channel network and onto adjacent tidal flats causes settling of mud out of suspension. Also, the fine-grained sediment settles on sand during low current-energy slackwater periods in a tidal cycle. Factors such as basin morphology, strength and dissipation pattern of the tidal currents, and vegetation further condition the distribution of sand and mud. This results in a complex spatial distribution of lithofacies which is difficult to model and predict.

Adequate modelling of the spatial arrangement of the sand-prone parts is especially relevant in hydrocarbon reservoirs in

this sedimentary environment, such as, e.g., the Tilje Formation (Pliensbachian, Early Jurassic) reservoirs in the Haltenbanken area offshore mid-Norway (Dreyer, 1992; Donselaar & Geel, 2003; Martinius et al., 2005), the Cook Formation (Early Jurassic) in the Oseberg Field, northern North Sea, offshore Norway (Donselaar et al., 2006), and The Lower Graben Formation (Late Jurassic) in the F3-FB Field, offshore the Netherlands (Wong, 2007). Well spacing is usually too large to capture all spatial sediment heterogeneity and to construct a unique, deterministic reservoir model. Instead, object-based stochastic modelling techniques are applied to generate multiple realisations of the spatial distribution to assess the uncertainty in sand-distribution and connectivity (Dubrule & Damsleth, 2001). However, if the parameters of the stochastic model are poorly known, the input distributions for these

parameters are usually chosen with wide ranges. The stochastic modelling exercise then inevitably results in a wide range of possible outcomes. Although this is exactly what stochastic modelling is supposed to do, it is clear that the range of possible outcomes will be narrower and the uncertainty better quantified when the ranges of the input parameters are better defined or estimated. Ideally, this is done by adapting the input distributions from analog, 'real-world' sediments. In a reservoir setting this is impossible because of the limited data density in the wide-spaced wells.

In the present paper the sparse data density problem is overcome by constructing the stochastic model from a highly data-constrained lithofacies architecture model of a tidal estuarine succession in the Holocene Holland Tidal Basin (HHTB) in the west of the Netherlands (Fig. 1). Stratigraphically, these deposits form the Beemster Deposits (Fig. 2; Westerhoff et al., 1987; Beets et al., 1996), now called the Wormer Member of the Naaldwijk Formation (Weerts et al., 2000). The deposits are in the shallow subsurface (down to 30 m depth) in a tectonically undisturbed area. The area is densely perforated with Cone Penetration Tests (CPT) and cored boreholes. The geological setting of the basin is well known from numerous publications (De Mulder & Bosch, 1982; Westerhoff et al., 1987; Van der Spek, 1994; Beets et al., 1996; Beets & Van der Spek, 2000; Beets et al., 2002). The data density allowed for the construction of a highly data-constrained facies architecture model that comprises size and shape data, directional trends and spatial relationships of the lithofacies associations (i.e., the building blocks of the model) that make up the tidal estuarine deposits (Donselaar & Geel, 2007).

The aim of this article is to assess the connectivity of the sand-prone sediments in the basin and its dependence on the modelling input parameters used (sediment body width and thickness). A sensitivity analysis will be performed with the drainable volumes as a sensitivity indicator.

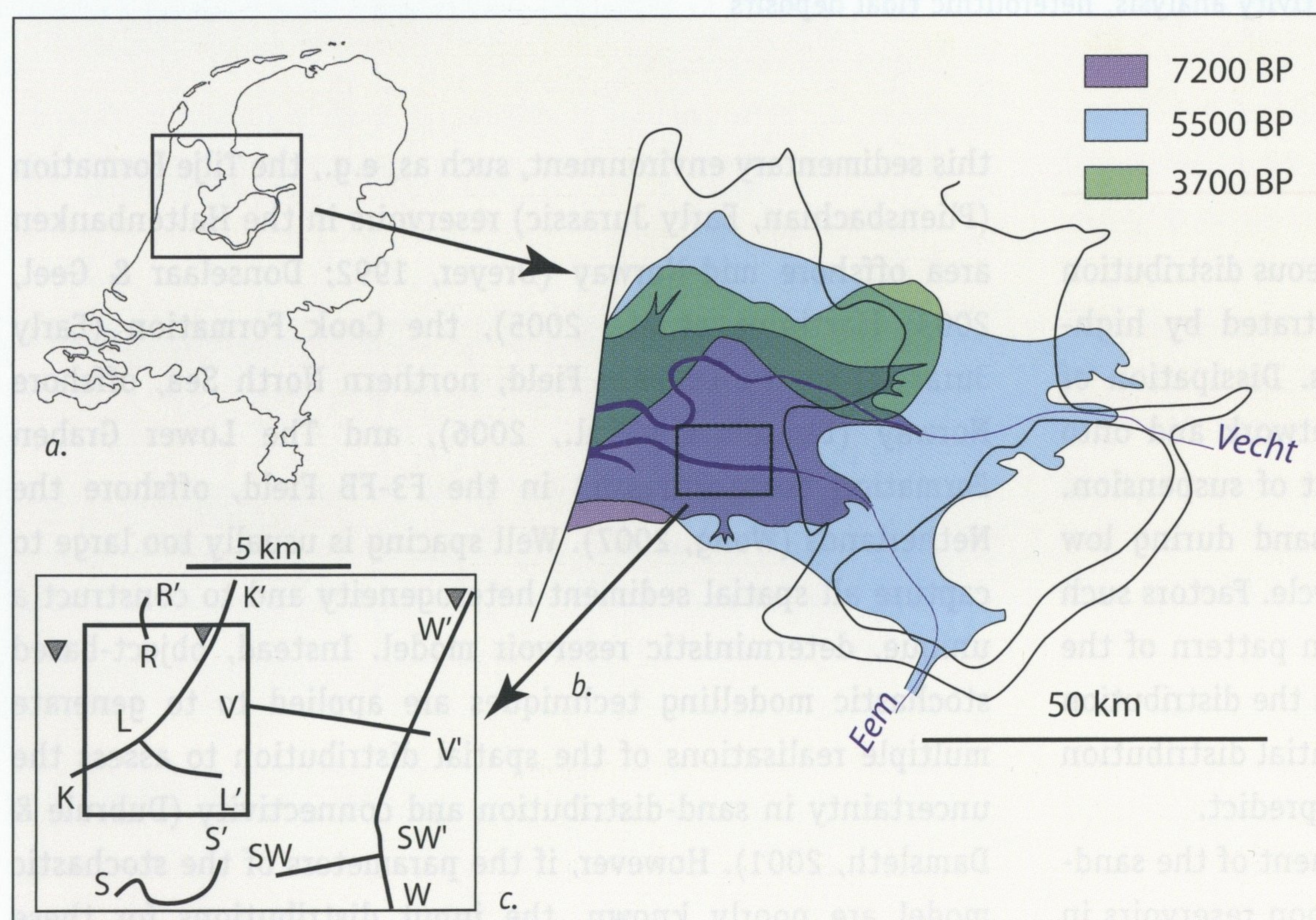


Fig. 1. a-b. Location of the Holocene Holland Tidal Basin (HHTB) in the west of the Netherlands; b. Development in space and time of the HHTB (modified from Van der Spek, 1994); c. Location map of CPT correlation lines (K-K', L-L', etc.) and cores (triangles) used to derive the size, shape and spatial position data used in this study. Small box: stochastic model area.

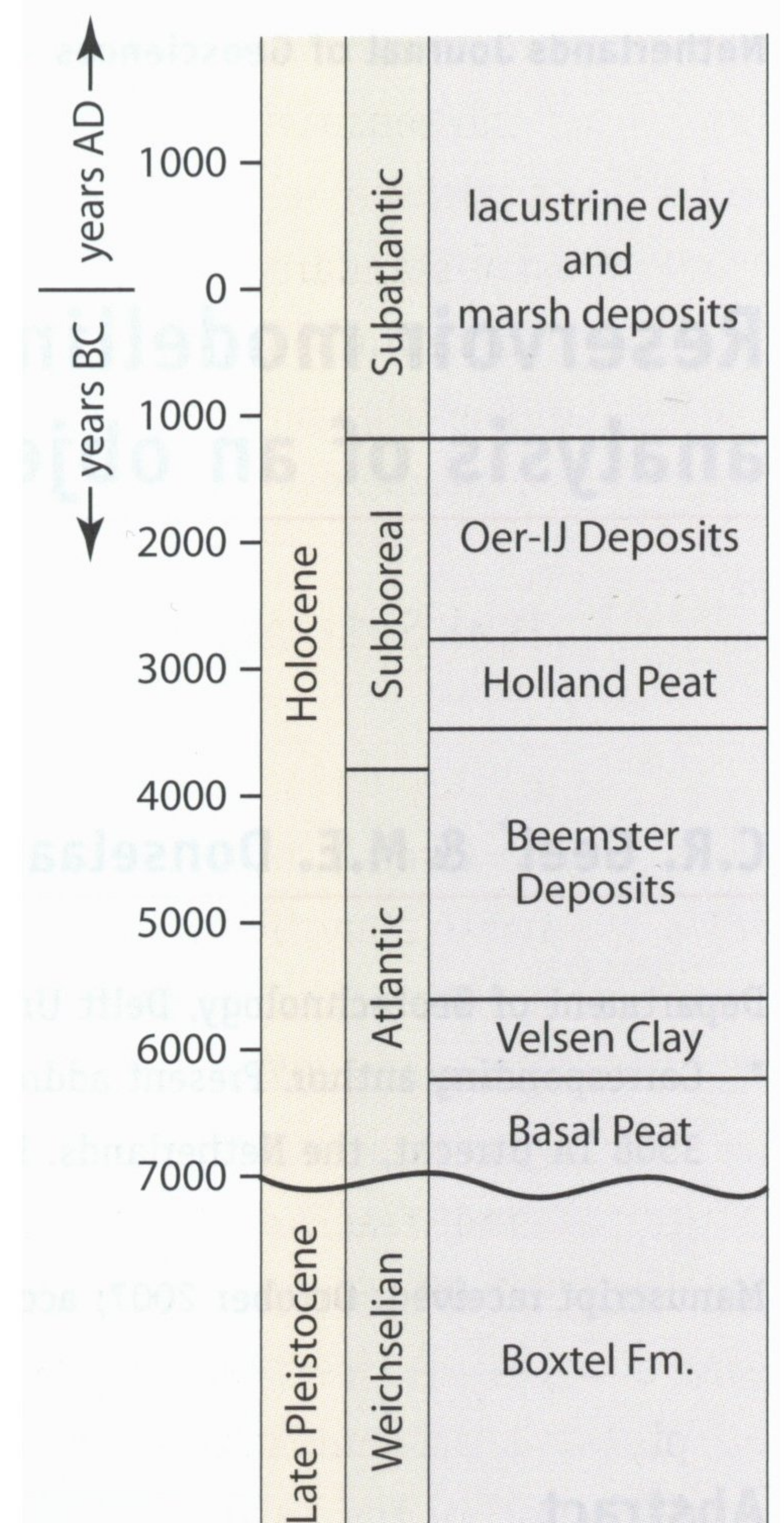


Fig. 2. Holocene stratigraphy column of the HHTB. Modified from Beets et al. (2002).

## Data and Methods

This study is based on a detailed facies architecture model of tidal estuarine deposits in the Holocene Holland Tidal Basin (HHTB). The model was established through the analysis and correlation of closely-spaced Cone Penetration Tests (CPT) and lacquer peels of undisturbed cores in an 11 by 14 km area (Donselaar & Geel, 2007). The size and shape data, directional trends and spatial relationships of the sedimentary facies types in the tidal basin were used to build an object-based stochastic reservoir model for the tidal basin fill in a smaller, 5 by 6 km area of the basin (Fig. 1). The smaller area was selected in such a way that the channel size in the along-flow direction

could be kept constant. The construction of the reservoir model and the sensitivity study were carried out with Roxar's STORM and RMS modelling software (Hardy & Hatløy, 2005). This industry-standard reservoir modelling package lacks a dedicated estuarine module. However, this has been solved by modifying the fluvial module of the package (see below: Stochastic object-based modelling).

## Geological Setting

The tidal estuary deposits formed during the Holocene glacio-eustatic sea-level rise by flooding of a westward-draining incised fluvial valley in the west of the Netherlands (Van der Spek, 1994; Beets & Van der Spek, 2000; Beets et al., 2002; Donselaar & Geel, 2007). Triggered by the high initial rate of Holocene sea-level rise (around 1 cm/yr) the basin gradually expanded and reached its largest extension of 2800 km<sup>2</sup> around 5500 BP (Fig. 1). The subsequent deceleration of the rate of sea-level rise changed the balance between sediment supply and accommodation increase and resulted in the gradual infill of the basin.

The base of the Holocene estuarine succession consists of a marsh deposit, the Basal Peat, formed on top of the Pleistocene

truncation surface and is covered with fine-grained, brackish water clay, the Velsen Clay. It is overlain by a sequence of sand, thinly bedded heterolithic and clay deposits, the Beemster Deposits that formed in a tidal estuarine environment (Westerhoff et al., 1987). These deposits are covered by clay and peat deposits of the Dunkerque Deposits and Holland Peat respectively, which formed as the tidal estuary silted up and converted to a freshwater marsh.

## Facies Architecture of the Beemster Deposits

The tidal estuarine Beemster Deposits comprises four lithofacies associations: (1) tidal channel sand, (2) sand-dominated heterolithic inter-tidal flat, (3) mud-dominated heterolithic inter-channel, and (4) fresh-water peat (Donselaar & Geel, 2007). The tidal channels built an intricate network of juxtaposed and vertically stacked sand bodies embedded in mud-dominated sub-tidal heterolithic and clay sediment (Fig. 3). The tidal channel sand bodies are lens-shaped in cross section, with a concave lower surface and flat upper surface. Channel sand body thickness is up to 6 m in the west and decreases to around 3 - 4 m in the east of the study area. Sand-dominated heterolithic tidal flat sediment bodies extend from the channel

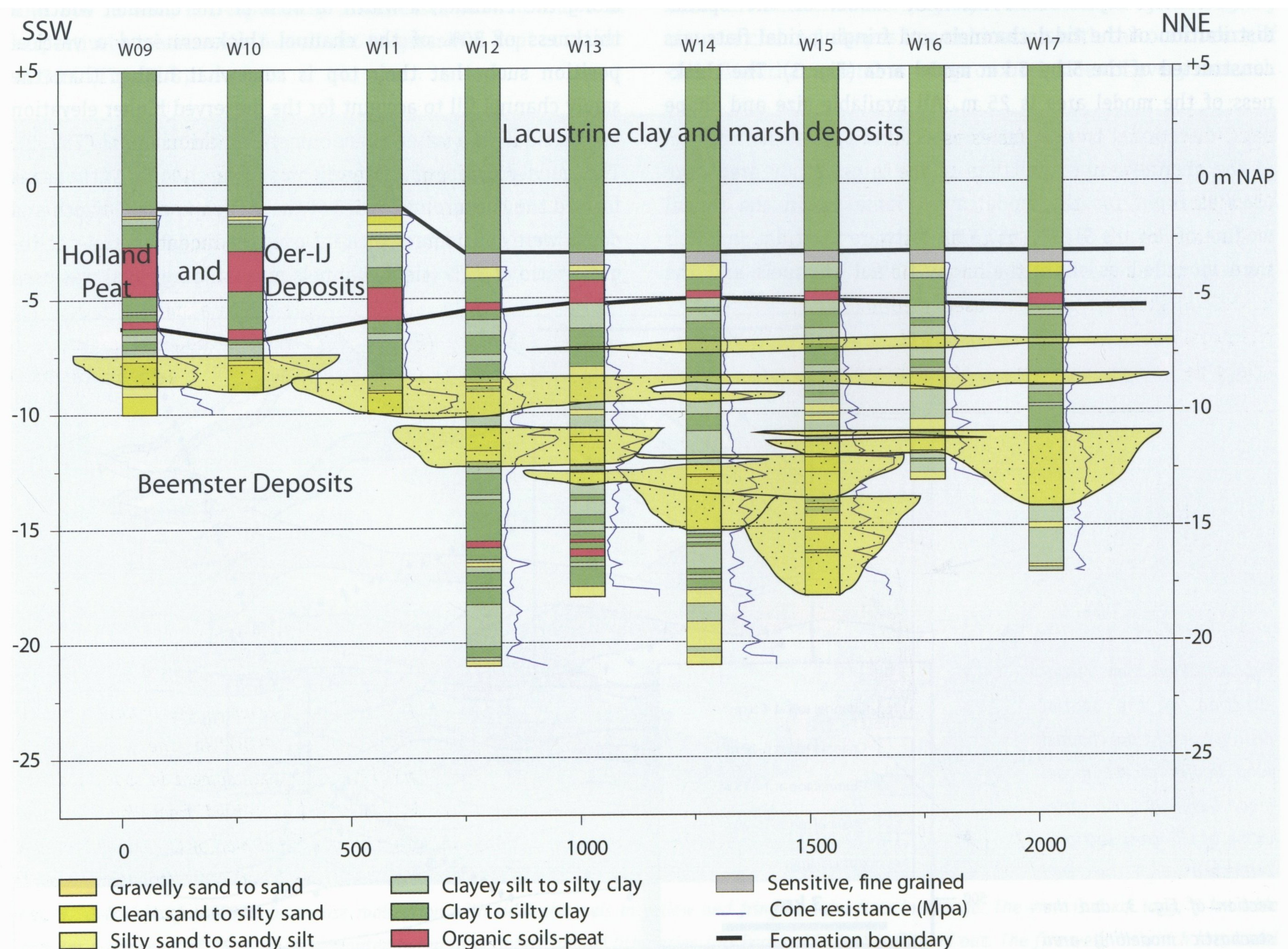


Fig. 3. CPT panel W-W'. See Fig. 1c for panel location.

sand bodies as sheet-shaped wings. The tidal flat deposits fringe the tidal channel sands along their entire length. The thickness of the tidal flat deposits ranges from less than a metre to several metres; the width varies from several hundred metres to more than one kilometre.

Plan view reconstruction based on the correlation of CPT cross-sectional panels illustrates that the tidal channel sand bodies have an east-west elongate, slightly sinuous ribbon shape (Fig. 4). The individual channel sand bodies are continuous over the length of the study area, i.e., their minimum length is 14 km. The tidal channel sand bodies bifurcate to the east and show a fractal pattern (c.f., Cleveringa & Oost, 1999). Width and thickness decrease upon bifurcation. Width values have an uncertainty because of the spacing of CPT log locations. Channel width attains a maximum of 1.3 km in the west and decreases to an average of 400 m in the east.

The mud-dominated inter-channel facies constitutes the bulk of the basin fill and is regarded the 'background' facies for modelling purposes. As such it has no size, shape, or orientation.

### Stochastic Object-based Modelling

A stochastic object-based reservoir model of the spatial distribution of the tidal channels and fringing tidal flats was constructed of the 5 by 6 km model area (Fig. 3). The thickness of the model area is 25 m. All available size and shape data, directional trends, net-to-gross and spatial distribution of the channels and tidal flats of the larger study area were used as input for the model area (Table 1). In the fluvial module of Roxar's STORM and RMS software the tidal channels were modelled as slightly sinuous fluvial channels and the

Table 1. a. STORM input parameters for tidal channel dimensions; b. STORM input parameters for tidal flat dimensions.

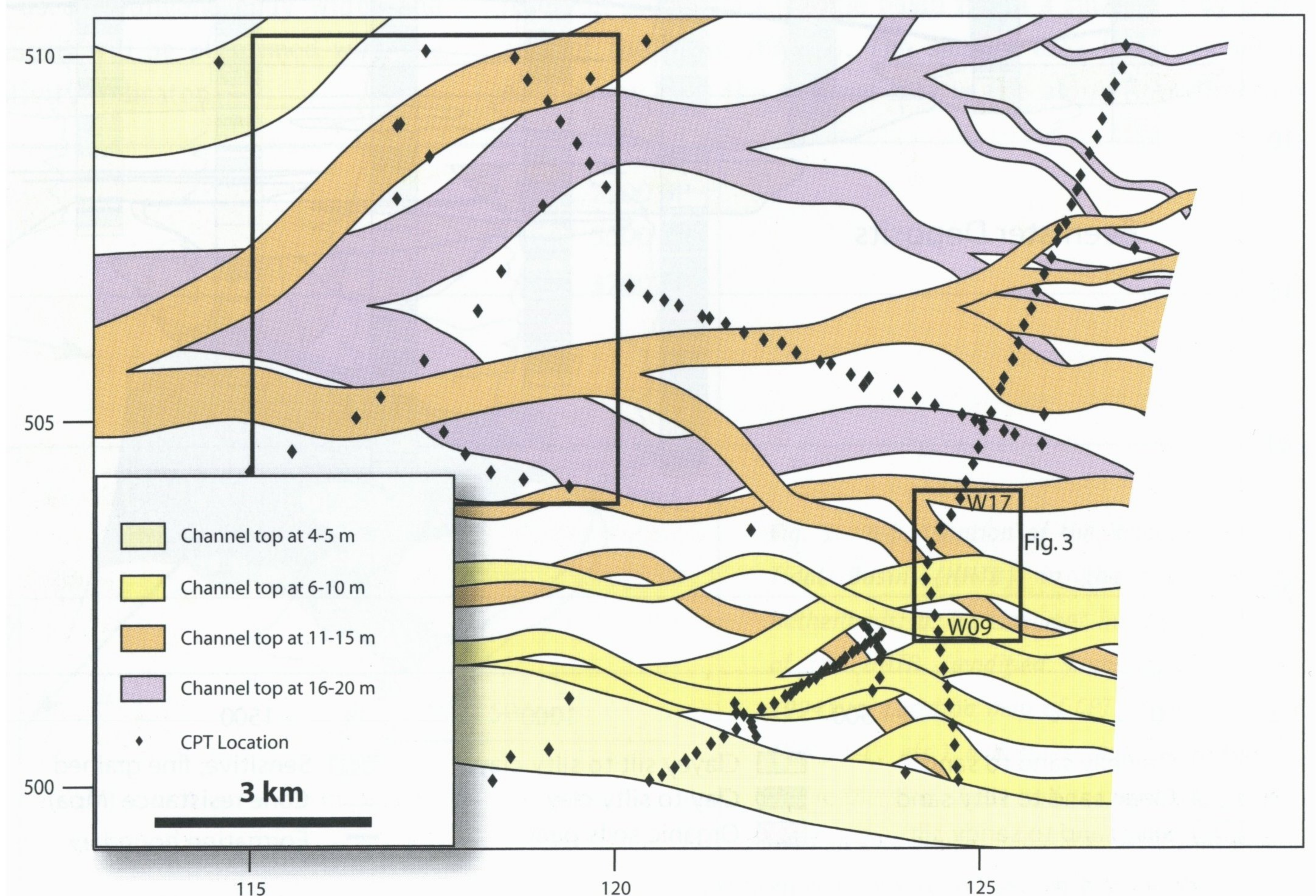
a. Tidal channel parameters	At top of zone	At bottom of zone
Av. width (m)	400	400
Std. dev. (+/-) width (m)	300	300
Av. thickness (m)	8	8
Std. dev. (+/-) thickness (m)	6	6

b. Tidal flat parameters	Width (m)	Thickness (m)
Expected value (relative to channel)	0.8	0.03
Std. dev.	0.01	0.01
Range	1000	

fringing tidal flats as crevasse splays. The tidal channels were modelled as a family of east-west oriented slightly sinuous, 400 m wide channels (*family* refers to model objects with a set of size and shape input parameters). Although the channels show a fractal pattern (Fig. 4), the size of the model area allows for the assumption of a constant channel width. Intertidal sand flats were defined as a family of channel-fringing sheets on both sides of the channel with an infinite length along the channel, a width of 80% of the channel width, a thickness of 30% of the channel thickness, and a vertical position such that their top is somewhat higher than the sandy channel fill to account for the preserved higher elevation of the tidal flats after abandonment of the channel (Fig. 5). The mud-dominated heterolithic inter-channel lithofacies formed the background facies of the model. Channel width and depth were considered constant over the model area. A net-to-gross ratio of 30% (tidal channels plus fringing flats) was used

Fig. 4. Plan view reconstruction of the spatial distribution of tidal channel sand bodies in the model area, based on the correlation of CPT cross sections. Indicated are the well section of Fig. 3, and the stochastic modelling area (large box).



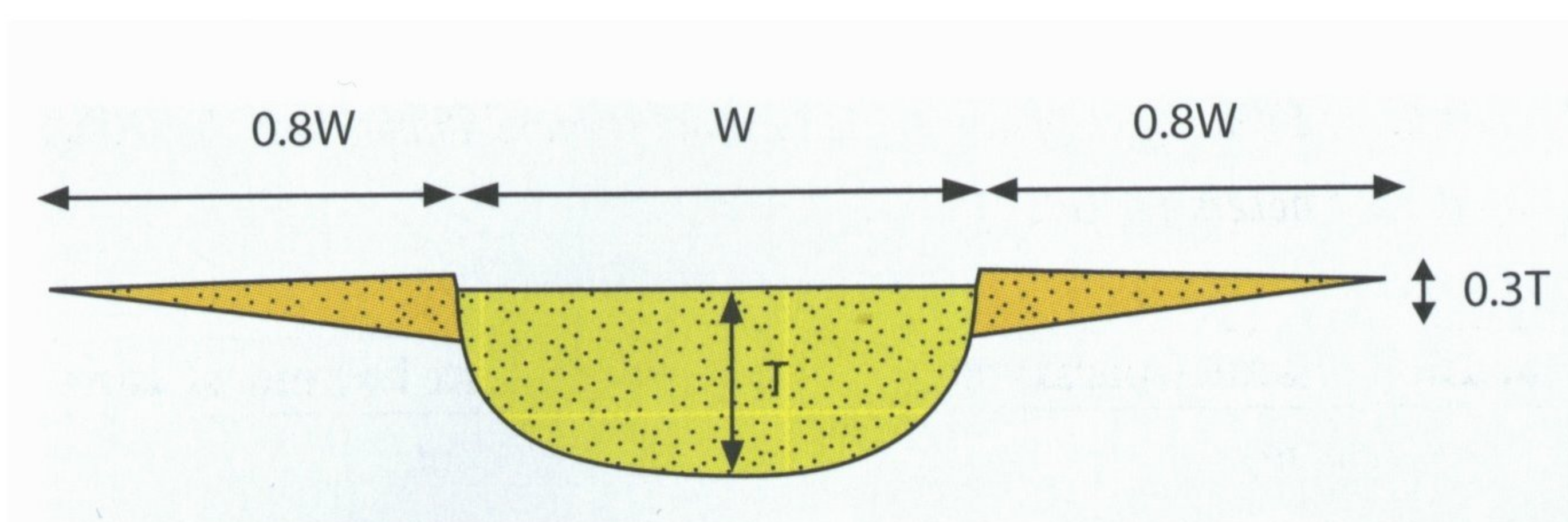


Fig. 5. Inter-tidal sand flat position relative to tidal channel.

as a stop criterion for the stochastic modelling process. The net-to-gross is the average measured value in all CPT logs. A truth case was constructed with use of all 25 available wells in the area. The well density strongly limits the stochastic freedom of the model and resulted in a highly data-constrained deterministic model (Fig. 6). However, in a reservoir setting the well spacing is large and therefore the channel width and thickness is difficult to estimate from these wells only. To accommodate for this uncertainty a number of realizations was generated with variable  $W/T$  and conditioned on five wells. CPT logs were used for this purpose. The average well spacing is 1.825 km and the wells line up in a NNE-SSW orientation (Fig. 6). The well spacing was chosen to approximate a typical offshore production well spacing, and the well-connecting line cuts the channel trend obliquely. Channel width was varied to 100 m and 800 m with corresponding thicknesses of 4 m and 8 m respectively, whereas the overall net-to-gross was kept constant at 30% (Figs 7, 8).

Model results show a large variety in reservoir architecture (Figs 6 - 8). To assess the dependency of the sand connectivity on the input parameters a sensitivity analysis was carried out. Connectivity calculations for the five wells were performed by computation of the drainable volumes per well with a given radius around the well. This radius can be considered as a cylindrical area around a well that can be drained in a certain amount of time, typically 5-30 years. It is controlled by a large number of factors, permeability being the most important one. A total of three cases were calculated with different width and thickness values: the base case, a case with smaller channels and one with larger channels (Figs 7, 8; Table 2). Four well radii were used: 200, 500, 800 and 1000 m (Fig. 9). Values are common in an oil reservoir setting. In addition, a theoretical value for every well radius was calculated using the volume of a cylinder with a height of 25 m (i.e., the model height) and a sand percentage of 30% to accommodate for the case where channel width and thickness ranges are not known and net-to-gross was extracted from well logs.

### Sensitivity Analysis Results and Discussion

The model output shows a high degree of connectivity between the individual channels (Fig. 6). This is caused by the slightly sinuous channel shapes in combination with the occurrence of tidal flats that extend as wings on both sides of every channel.

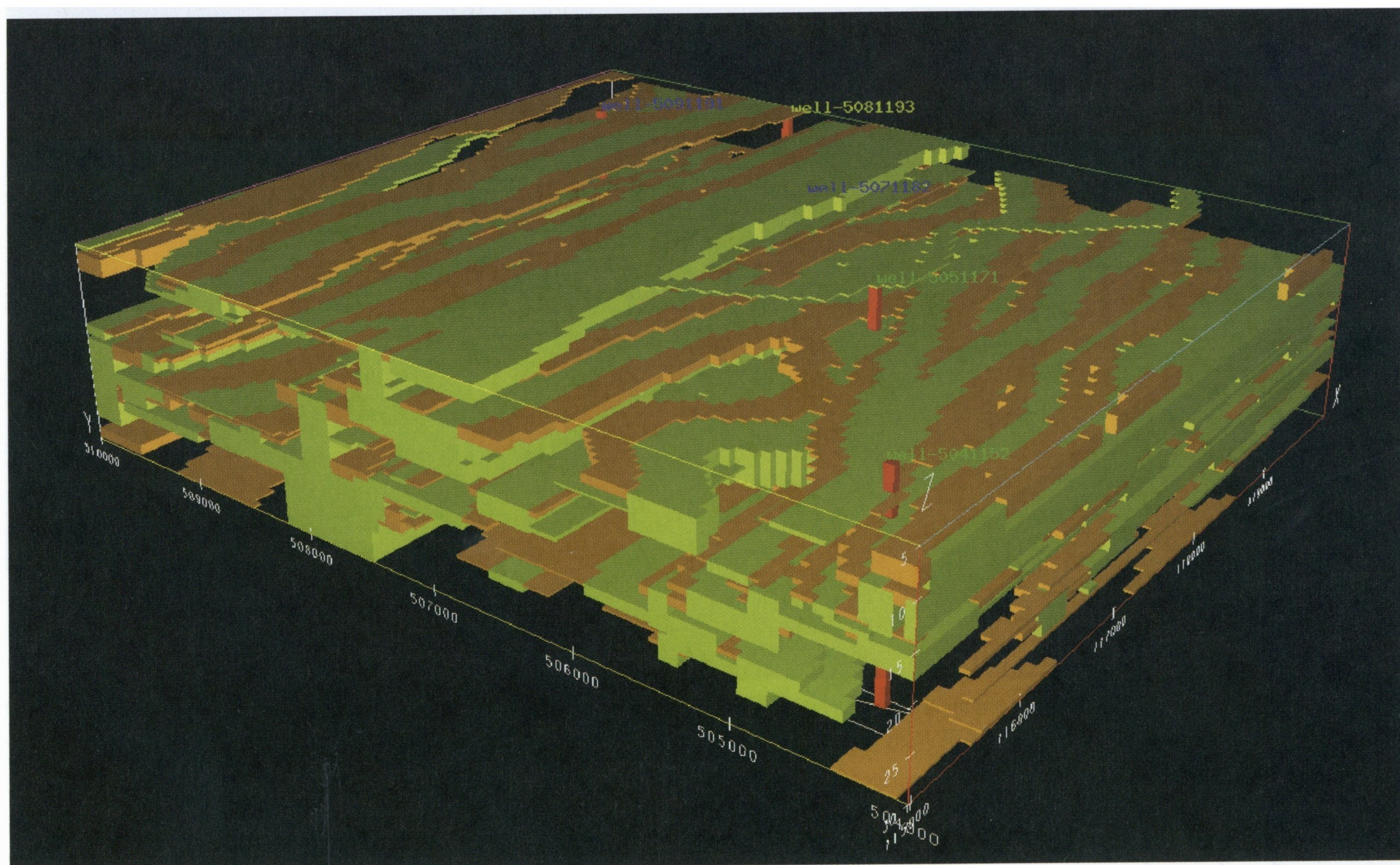


Fig. 6. 3-D view of a STORM base case realization with tidal channels in yellow and fringing tidal flats in orange. The view is 6 km long, 5 km wide and has a thickness of 25 m. Mud-dominated heterolithic inter-channel lithofacies (background facies) is filtered out. The five wells on which the model is conditioned are shown.

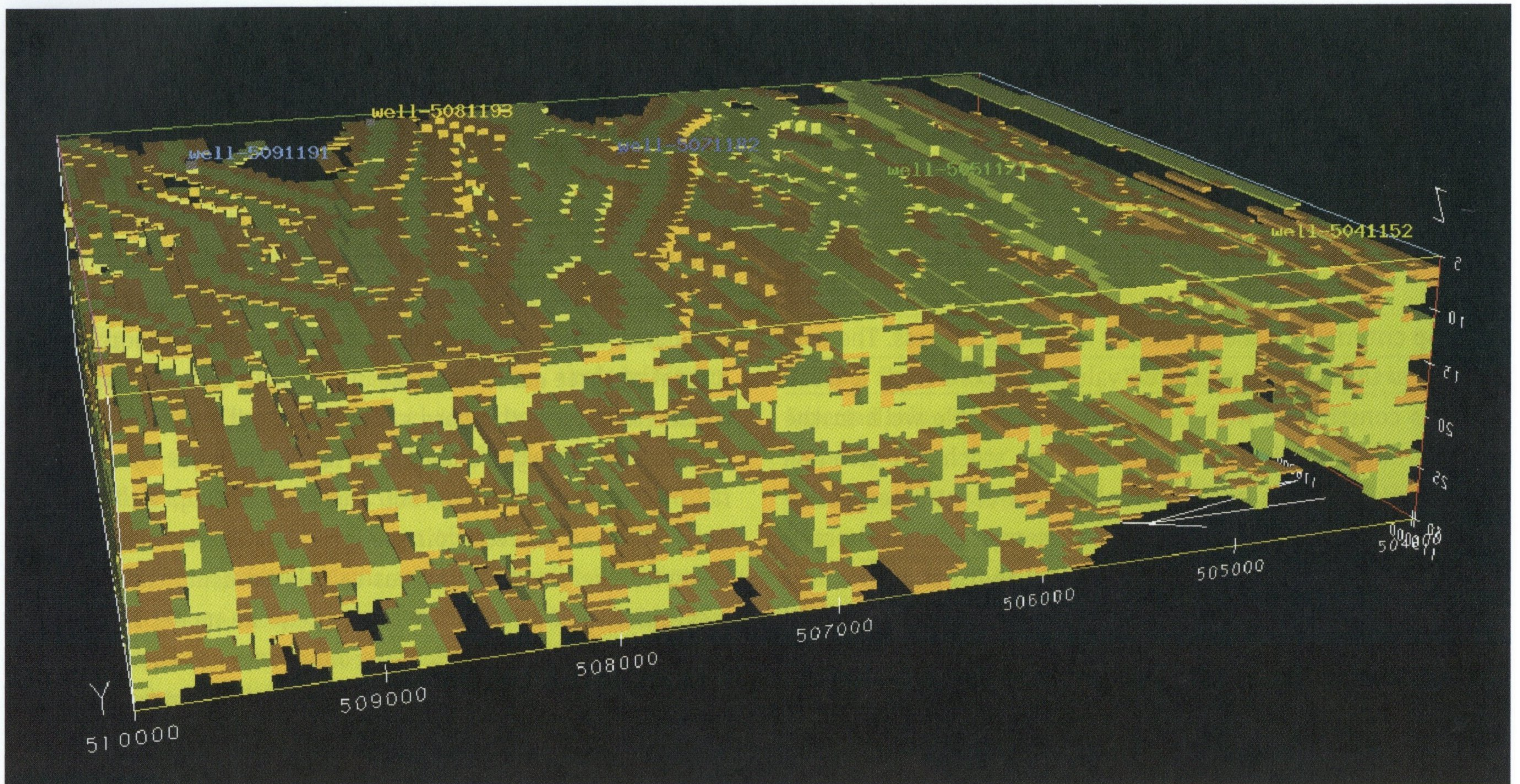


Fig. 7. 3-D view of a STORM realization with 100 m wide channels. Model size and colours as in Fig. 6.

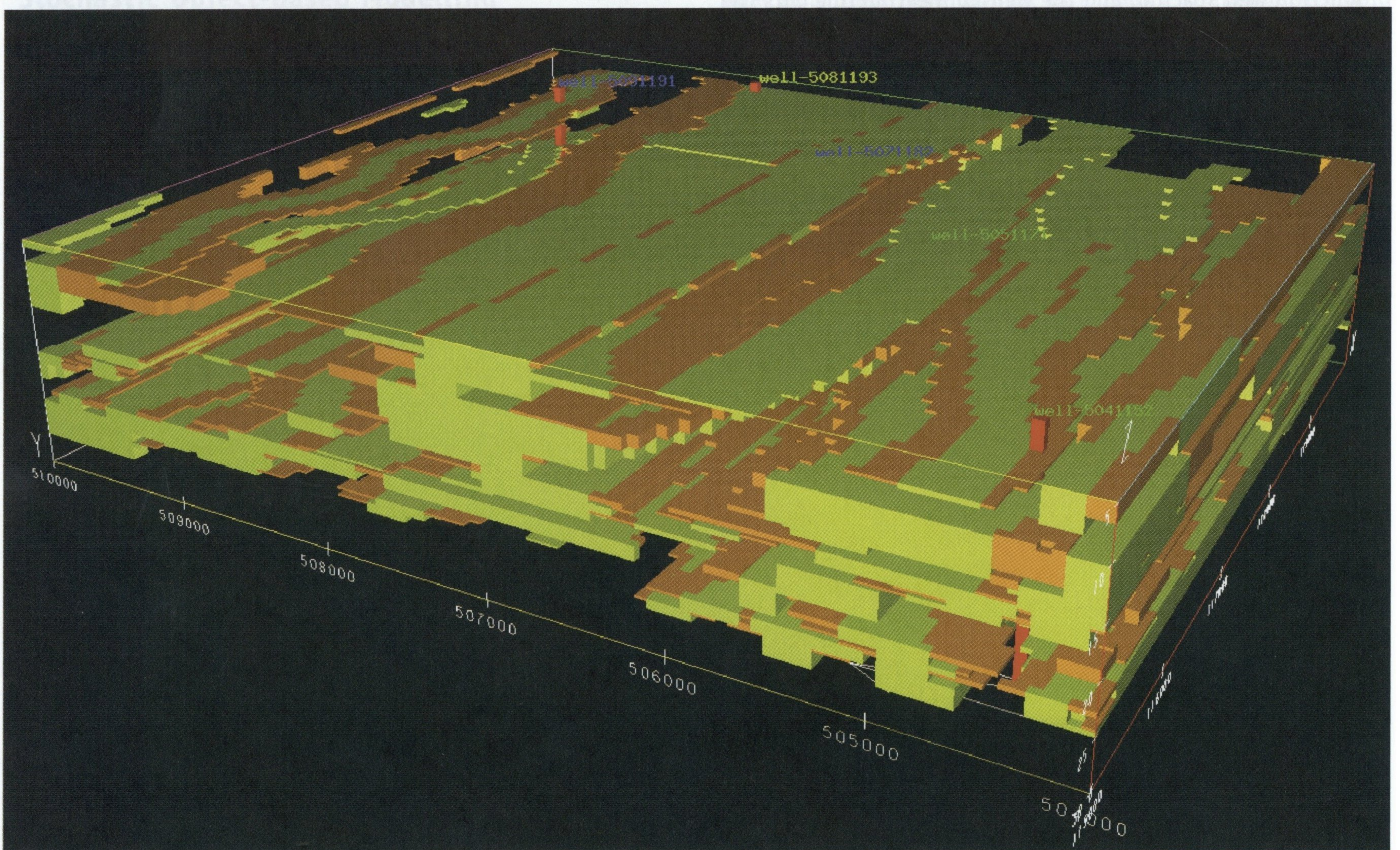


Fig. 8. 3-D view of a STORM realization with 800 m wide channels. Model size and colours as in Fig. 6.

The results indicate that for a large well drainage radius the tidal channel width hardly influences the drainable volume (Table 3, Fig. 10). For a small well drainage radius however, the difference in drainable volumes between the narrowest and the widest channel scenarios is 28%. The combination of well drainage radius and tidal channel width thus seems a

major controlling factor in the ultimate recovery of heterolithic tidal reservoirs. Furthermore, the results show that experimentally determined drainable volumes yield lower values than the theoretical value. In the experimental cases the wells do not necessarily penetrate the reservoir at the optimal channel stacking and the sand percentage will

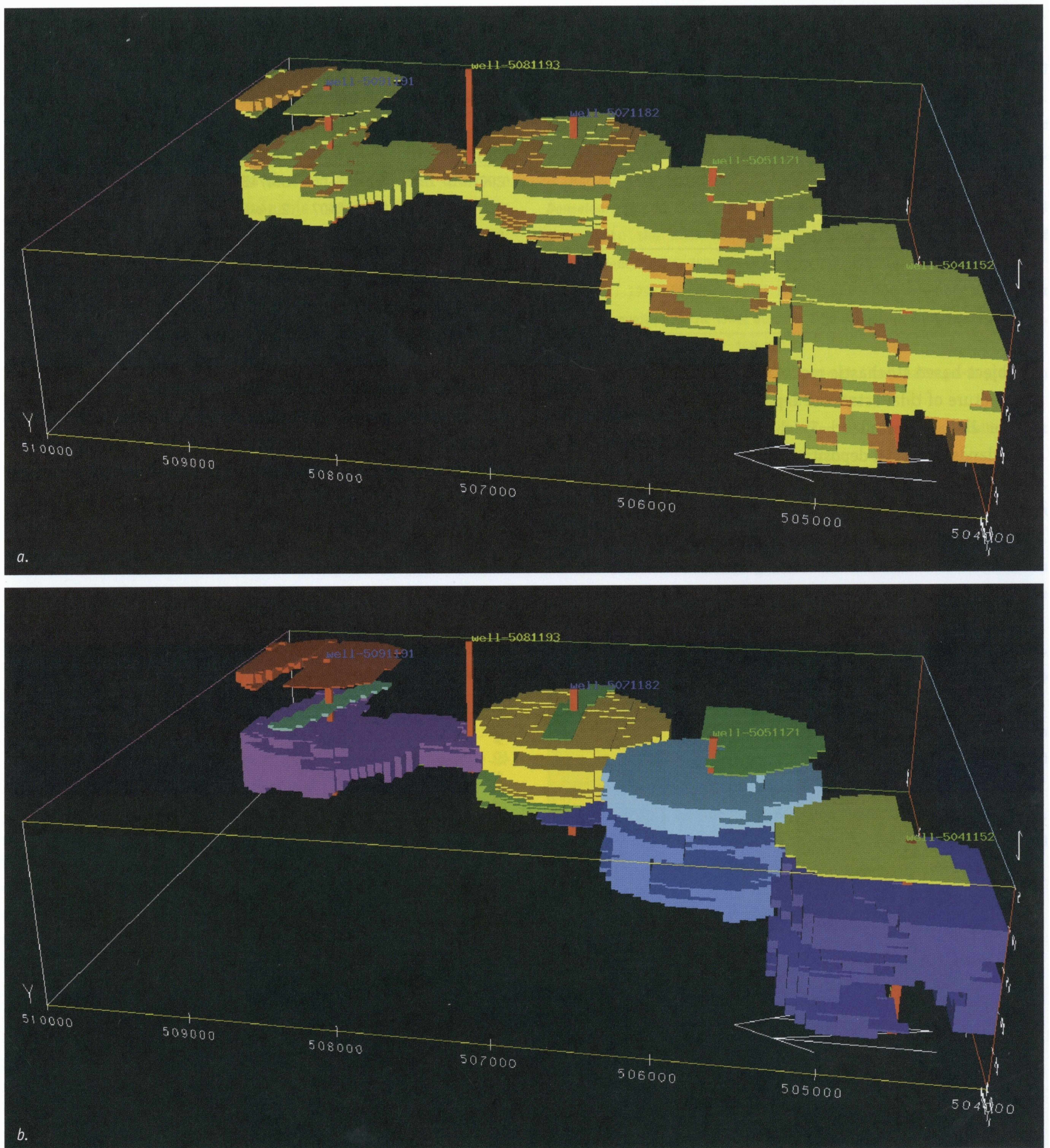


Fig. 9. Realization of the connected volumes in the 800 m wide channel case; a. Shown are the parts of the tidal channels (yellow) and tidal flats (orange) connected to the wells, at a well radius of 800 m. Model size and colours as in Fig. 6; b. Individual drainable sand volumes connected to a well.

therefore be lower than the 30% sand that is fixed in the theoretical case. The variability in sand percentage is clearly shown in Fig. 9 where the well on the left has a lower sand percentage than the other wells.

The fact that the experimental results of connected volume do not differ significantly for different channel widths for the majority of the well radii (Fig. 10) may seem counterintuitive, because a higher degree of connectivity would be expected for

wider channels. However, the high degree of connectivity is caused by the tidal flat 'wings' that extend from every channel. Although they are volumetrically not very important because of their small thickness, they increase the channel width by a factor 2.6 and may thus effectively establish the lateral connectivity between channels (Fig. 9). A similar result, albeit in a somewhat different setting was achieved by Brandsaeter et al. (2001).

Table 2. Width and thickness input values of the cases used in the sensitivity analysis. The theoretical case consists of a cylinder with a sand percentage of 30%.

Cases	Width (m)	Thickness (m)
Truth case	400	8
Small channels	100	4
Wide channels	800	8
Theoretical	-	-

## Conclusions

An object-based stochastic model was established of the facies architecture of tidal estuarine deposits (the Beemster Deposits) in the Holocene Holland Tidal Basin in the west of the Netherlands. The tidal deposits comprise four lithofacies associations: (1) tidal channel sand, (2) sand-dominated heterolithic inter-tidal flat, (3) mud-dominated heterolithic inter-channel, and (4) fresh-water peat. Plan view reconstruction of the tidal

Table 3. Drainable volumes (m<sup>3</sup>) from five wells, calculated for sixteen cases: four different tidal channel width/thickness cases, each with four different well radii.

Well Radius (m)	Base case	Small channels	Wide channels	Theoretical
200	3.940E+06	3.474E+06	4.444E+06	4.710E+06
500	2.414E+07	2.144E+07	2.414E+07	2.940E+07
800	6.130E+07	5.640E+07	5.763E+07	7.540E+07
1000	9.028E+07	8.120E+07	8.964E+07	1.178E+08

channel sand bodies in the study area show the east-west elongated, slightly sinuous tidal channel pathways with a bifurcating pattern towards the east (landward). The size, shape and spatial distribution data that served as input for the stochastic model were derived from correlation panels of closely-spaced CPT logs. The high data density of the CPT logs (log spacing 100 - 300 m) constrained the stochastic model. The model output showed a high connectivity between the channel sands. The connectivity is established by the combination of

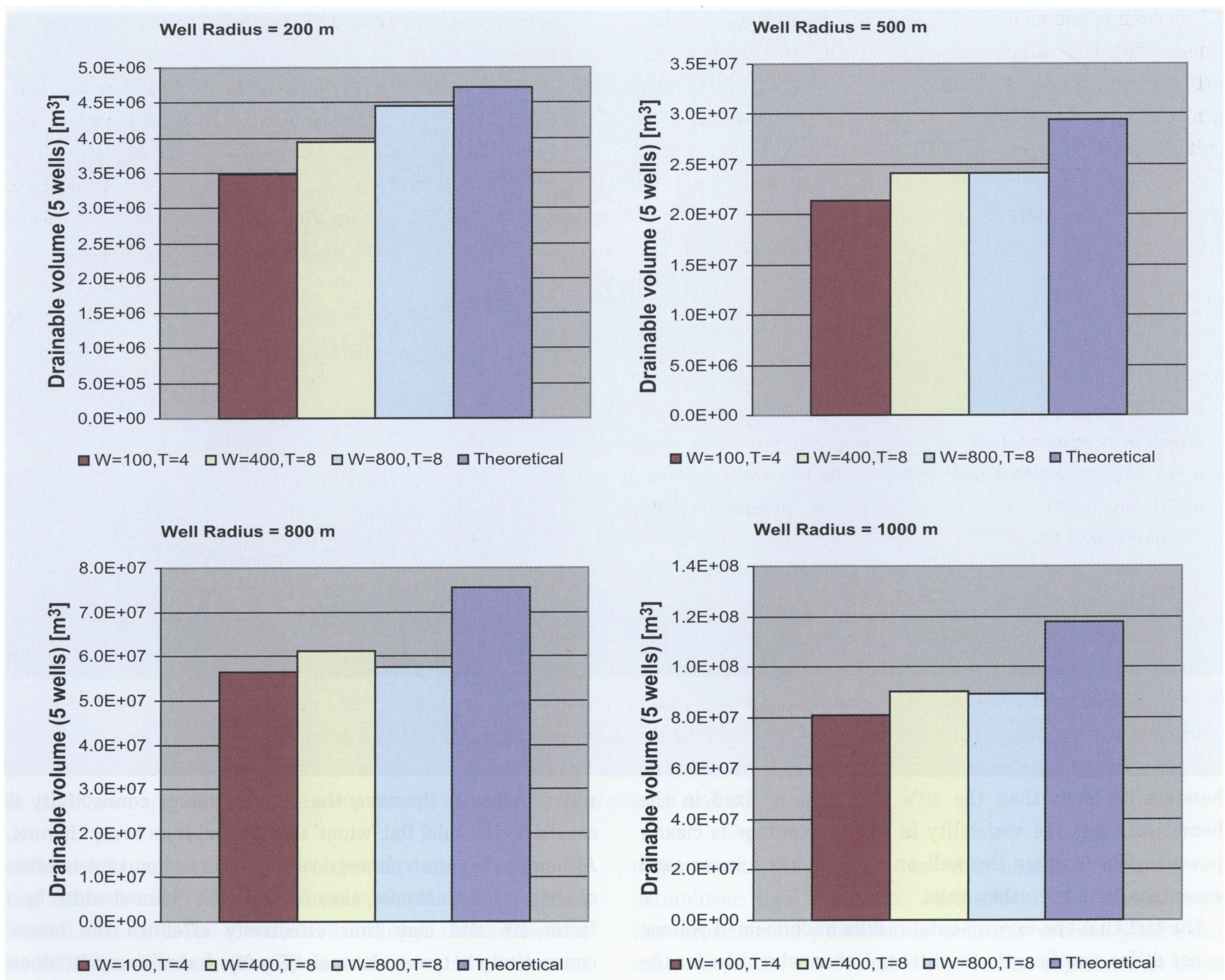


Fig. 10. Results of the drainable volume sensitivity analysis for different well drainage radii and channel widths.

slightly sinuous channel shapes in combination with the occurrence of sand-dominated tidal flat deposits that extend as wings on both sides of every channel. The sensitivity of the model to the input parameters was analysed with the use of varying tidal channel width and thickness values and calculating the connected volume per well for the different scenarios. The results indicate that for a small well drainage radius the difference in drainable volumes between the narrowest and the widest channel scenarios is large (28%), and that for a large well drainage radius the tidal channel width hardly influences the drainable volume. The experimental cases all yielded lower connected volume values than a theoretical case with a fixed sand percentage. The differences are explained by spatial variability in channel sand stacking that yield lower connected volume values for the experimental cases. The sensitivity analysis confirmed the importance of sand-dominated tidal flats in improving lateral connectivity.

## Acknowledgements

The authors are indebted to Frans Otten (now at Roxar) for the CPT processing and analysis, and for setting up the correlation panels. Financial support for the study was provided by Fortum Petroleum AS. We thank Torgeir Vinje (then at Fortum Petroleum) for initiating and supporting the project. TNO Built Environment and Geosciences, *Geological Survey of the Netherlands* is acknowledged for access to the Holocene tidal basin data. The authors are grateful to NJG reviewers Poppe de Boer and Djin Nio for their constructive comments.

## References

- Beets, D.J., De Groot, Th.A.M. & Davies, H.A.**, 2002. Holocene tidal back-barrier development at decelerating sea-level rise: a 5 millennia record, exposed in the western Netherlands. *Sedimentary Geology* 158: 117–144.
- Beets, D.J., Roep, Th.B & Westerhoff, W.E.**, 1996. The Holocene Bergen Inlet: closing history and related barrier progradation. *Mededelingen Rijks Geologische Dienst N.S.* 57: 97–131.
- Beets, D.J. & Van der Spek, A.J.F.**, 2000. The Holocene evolution of the barrier and the back-barrier basins of Belgium and the Netherlands as a function of late Weichselian morphology, relative sea-level rise and sediment supply. *Netherlands Journal of Geosciences* 79: 3–16.
- Brandsaeter, I., Wist, H.T., Naess, A., Lia, O., Arntzen, O.J., Ringrose, P.S., Martinus, A.W., & Lerdahl, T.R.**, 2001. Ranking of stochastic realizations of complex tidal reservoirs using streamline simulation criteria. *Petroleum Geosciences* 7: S53–S63.
- Cleveringa, J. & Oost, A.P.**, 1999. The fractal geometry of tidal-channel systems in the Dutch Wadden Sea. *Geologie en Mijnbouw* 78: 21–30.
- De Mulder, E.F.J. & Bosch, J.H.A.**, 1982. Holocene stratigraphy, radiocarbon datings and paleogeography of central and northern North-Holland (the Netherlands). *Mededelingen Rijks Geologische Dienst* 36: 113–160.
- Donselaar, M.E., Dalman, R.A.F., Dreyer, T., Petersen, S.A., Thomassen, R.A.J. & Toxopeus, G.**, 2006. Reservoir Architecture Modeling of the Cook Formation, Oseberg Field, Offshore Norway: Integrated Analysis of Core, Well Log and Seismic Data. AAPG 2006 Annual Meeting, Houston, Texas, April 9 - 12, 2006.
- Donselaar, M.E. & Geel, C.R.**, 2003. Reservoir architecture model for heterolithic tidal deposits. 65rd EAGE Conference & Technical Exhibition – Stavanger, Norway, 2 - 5 June 2003.
- Donselaar, M.E. & Geel, C.R.**, 2007. Facies architecture of heterolithic tidal deposits: the Holocene Holland Tidal Basin. *Netherlands Journal of Geosciences* 86/4: 389–402.
- Dreyer, T.**, 1992. Significance of tidal cyclicity for modelling of reservoir heterogeneities in the lower Jurassic Tilje Formation, mid-Norwegian shelf. *Norsk Geol. Tidsskrift* 72: 159–170.
- Dubrule, O., & Damsleth, E.**, 2001. Achievements and challenges in petroleum geostatistics. *Petroleum Geosciences* 7: S1–S7.
- Hardy, D. & Hatløy, A.**, 2005. The changing face of reservoir modelling. *First Break* 23, 63–66.
- Martinus, A.W., Ringrose, P.S., Brostrøm, C., Elfenbein, C., Næss, A. & Ringås, J.E.**, 2005. Reservoir challenges of heterolithic tidal sandstone reservoirs in the Halten Terrace, mid-Norway. *Petroleum Geoscience* 11: 3–16.
- Van der Spek, A.J.F.**, 1994. Large-scale evolution of Holocene tidal basins in the Netherlands. Published Doctorate thesis, Utrecht University, the Netherlands: 191 pp.
- Weerts, H.J.T., Cleveringa, P., Ebbing, J.H.J., Lang, F.D. & Westerhoff, W.E.**, 2000. De lithografische indeling van Nederland. Formaties uit het Tertiair en kwartair. TNO-NITG rapport 00-95-A. TNO-NITG, Utrecht: 38 p.
- Westerhoff, W.E., De Mulder, E.F.J. & De Gans, W.**, 1987. Toelichting bij de geologische kaart van Nederland 1:50.000: Blad Alkmaar West (19W) en Blad Alkmaar Oost (19O). Rijks Geologische Dienst, Haarlem: 227 pp.
- Wong, Th.E.**, 2007. Jurassic. In: Wong, Th.E., Batjes, D.A.J., De Jager, J. (eds), *Geology of the Netherlands*. Royal Netherlands Academy of Arts and Sciences: 107–125.